

Biophysical Journal, Volume 99

Supporting Material

High and low mobility stages in the synaptic vesicle cycle

Dirk Kamin, Marcel Lauterbach, Volker Westphal, Jan Keller, Andreas Schoenle, Stefan Hell,
and Silvio Rizzoli

Supporting Material

Supporting Materials and Methods:

Antibodies. The following antibodies were used for live cell imaging (STED and FRAP): monoclonal mouse antibodies 604.2 against the luminal domain of the synaptic vesicle protein synaptotagmin, and monoclonal mouse antibodies 604.2 directly labeled with Oyster-550 (from Synaptic Systems, Göttingen, Germany); Atto647N-labeled anti-mouse Fab fragments from donkey or goat (AffiniPure Fab fragments from Jackson ImmunoResearch Laboratories, West Grove, PA; organic fluorophore Atto647N from ATTO-TEC, Siegen, Germany). Labeling with Atto647N was performed as described previously (1). Antibodies for immunostaining were as follows: anti-Synaptophysin, anti-Clathrin light chain and anti-SNAP-25 polyclonal rabbit antibodies (G96 (2), Clc (3) and casanova (4); kind gifts from R. Jahn, Max Planck Institute for Biophysical Chemistry, Göttingen, Germany). Anti-alpha-Tubulin, anti-Amphiphysin, anti-GluR1 (AMPA1), anti-Rab3, anti-Synapsin 1, 2, anti-Munc13-1 and anti-Bassoon: all polyclonal rabbit antibodies (all from Synaptic Systems, Göttingen, Germany); see the web-site of Synaptic Systems for details on antibody specificity; Cy2-, Cy3-, Cy5-conjugated goat anti-rabbit IgG and Cy5-conjugated goat anti-mouse IgG (all AffiniPure, Jackson ImmunoResearch Laboratories, West Grove, PA). Mitotracker Green FM was obtained from Invitrogen.

Materials. Black widow spider venom (BWSV, Sigma Aldrich) was prepared as stock solution in calcium-free Tyrode buffer (1 mM EGTA) at 1 pair of glands/ml, and was used in the same buffer at a 1:4 dilution. BWSV incubation was performed for 15 minutes (37°C) before vesicle labeling. Caffeine (Sigma Aldrich) was used at 1 mM, and applied for 5 minutes at room temperature in Tyrode buffer without divalents (5 mM EGTA). Tetrodotoxin was obtained from Sigma Aldrich and used as indicated in the text.

Microscopy. STED microscopy was performed as previously described (5), using a home-built setup. Pulsed excitation (635 nm for the Atto647N, LDH-P-635, PicoQuant, Berlin, Germany and 490 nm for the Mitotracker, PicoTA 490, PicoQuant) and STED (750 nm, MaiTai Ti:Sapphire-Laser, Newport, Irvine, CA) beams passed a resonant mirror (SC-30, EOPC, Glendale, NY) for one axis beam scanning. They were focused into the sample by the objective (NA = 1.4 oil immersion, HCX PL AP, Leica). Focal peak intensities applied were 3.5-6, 0.08 and 400 MW/cm² for red excitation, blue excitation and the depletion beam, respectively. A piezo stage (733-3DD and E-710, Physik Instrumente, Germany) provided the second lateral axis and the axial scanning of the sample. The fluorescence light was bandpass filtered (675±30 nm for the red channel, 530±40 nm for the blue channel, AHF, Tübingen, Germany) and recorded by two avalanche photo diodes (SPCM-AQR13, Perkin Elmer). The spatial zero in the STED focus was accomplished by a vortex phase plate (VPP-A1, RPC Photonics, Rochester, NY) in the collimated STED beam path. Samples were imaged at 28 frames per second within 2 to 30–40 minutes after staining. Several movies were recorded from each sample. For display, the STED images were filtered by convolution with a Gaussian function of 80 nm full width at half maximum (except for Fig. 1 B, where no filtering was applied).

STED Microscopy data analysis. The vesicles were localized as described in the Methods part of the main text. All localized objects were then tracked as described previously (5), using the algorithm of Crocker and Grier (6). In brief, for each possible assignment of particles from one frame to the next the distance each particle travelled is calculated. The algorithm finds the assignment that minimizes the sum of squares of these distances. We imposed a maximum speed of 8.3 nm/ms (20 pixels/frame) beyond which particles were considered unmatched and entered with a penalty. Because tracking is generally prone to errors in dense samples, we use the median for the quantification of the mobility, which is less sensitive to a few false assignments. Using this approach differences in the speeds were well resolved between

different experiments, while the absolute values may not be perfect estimates for the actual movements. Even fixed samples show a residual average movement due to noise in the position estimation. Binning for the histograms was slightly randomized to avoid artifacts stemming from the fact that object positions are preferentially assigned to pixel centers.

Note that Matlab particle tracking codes can be downloaded from the web-site of Daniel Blair (Georgetown University) and Eric Dufresne (Yale University): <http://physics.georgetown.edu/matlab/>. An excellent tutorial on tracking particles with Matlab can be obtained from the same web-site.

“Hot spot” analysis (Fig. 2) was performed as described earlier (5).

Conventional imaging (confocal) data analysis. Line profile correlation analysis: lines along the axons were drawn manually in the synaptotagmin (red) channel, and the pixel intensities along the line were obtained for both the synaptotagmin and the protein of interest (green) channels; the Pearson’s correlation coefficient was then calculated. For Fig. S5, a similar procedure was followed; the immunostaining was performed in two steps: the synaptotagmin surface pool was immunostained in absence of permeabilization, followed by detergent treatment (Triton X-100, 0.1%) and immunostaining for clathrin and amphiphysin.

FRAP data were analyzed as follows: the movie frames were aligned by an automated routine in Matlab, and regions of interest were defined manually for the bleached spot and for several control areas. The average intensity within each area was determined for each frame of the movie. The average reduction in intensity in the control areas during movie acquisition (i.e. bleaching during image capture) was calculated, and the FRAP curve was normalized accordingly.

For calculating difference image values (Fig. 4), each frame of a movie was subtracted from the subsequent frame. We then calculated the mean of the absolute pixel values in the difference image, and expressed it as percentage of the mean pixel value in the original movie frame. The procedure was repeated for all movie frames. The plots were smoothed by applying a 15 frame moving average.

Endocytosis measurements were performed as follows: neuronal cultures (control, or treated with caffeine or BWSV) were incubated on ice with an Oyster-550-labeled variant of the anti-synaptotagmin antibody 604.2. They were then fixed after different incubation times and immunostained (without permeabilization) with a Cy5-labeled secondary anti-mouse antibody, which thus recognized specifically the surface synaptotagmin pool. We then measured the relative intensity of the surface synaptotagmin staining (Cy5) to the total synaptotagmin staining (Oyster-550). The results were expressed as percentage of the initial condition (no incubation before fixation).

Supporting Figures:

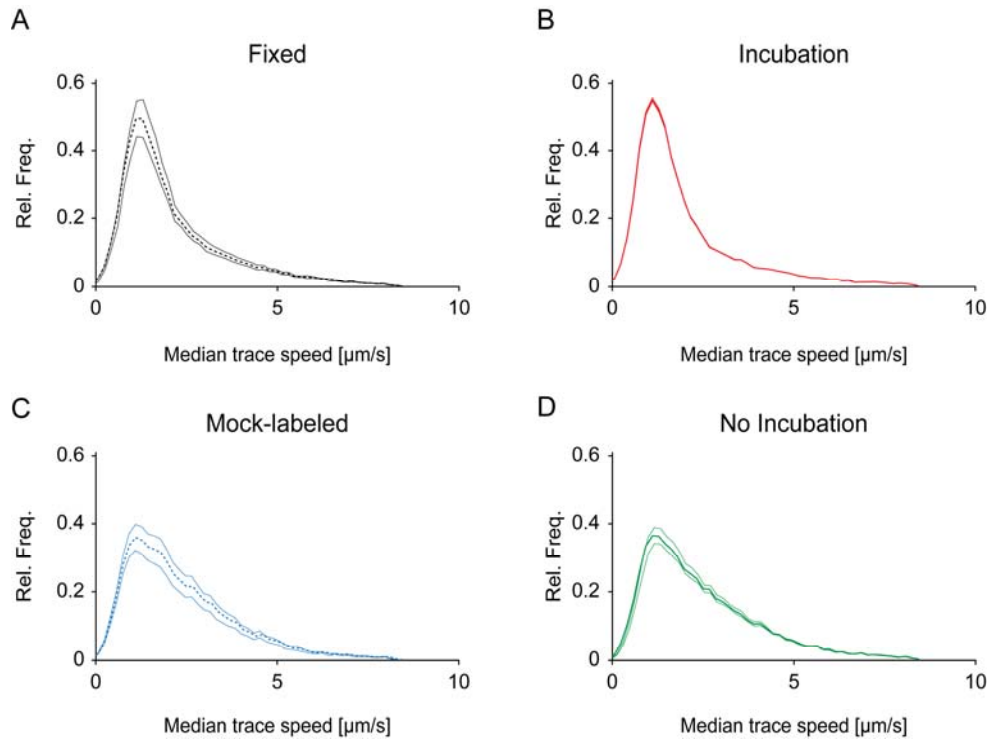


Figure S1: “Synaptic vesicle movement statistics”

(A)-(D) The histograms from Fig. 1 *F*, shown independently, indicating the standard error of the mean.

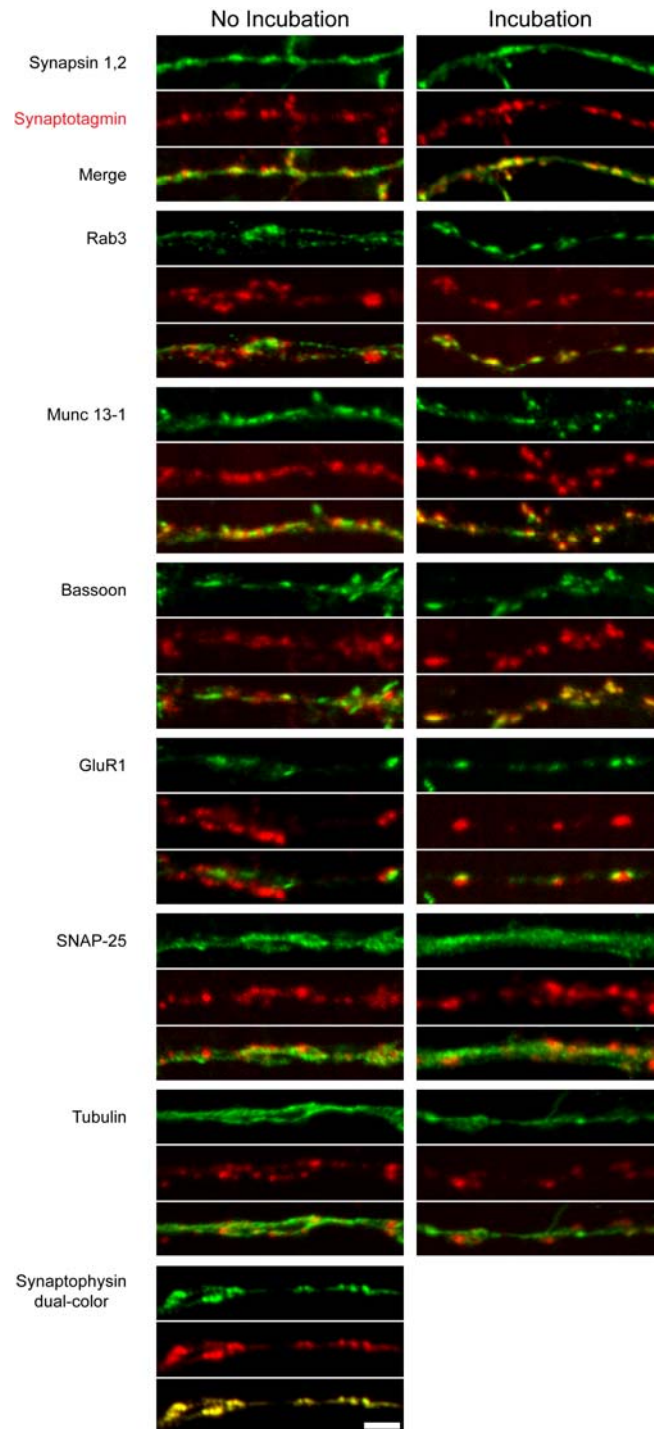


Figure S2: “Colocalization of newly endocytosed and incubated synaptic vesicles with different neuronal markers”

Living primary cultured hippocampal neurons were stained against synaptotagmin (shown in red) as described in Methods, and fixed with paraformaldehyde (4% in PBS) either after a 20-minute rest period at room temperature (No Incubation) or after incubation for two hours at 37°C (Incubation). The neurons were afterwards immunostained (after Triton X-100 permeabilization) against different proteins of interest (shown in green), including synaptic vesicle markers or active zone markers. Imaging was done by confocal fluorescence microscopy. Scale bar 2.5 μm .

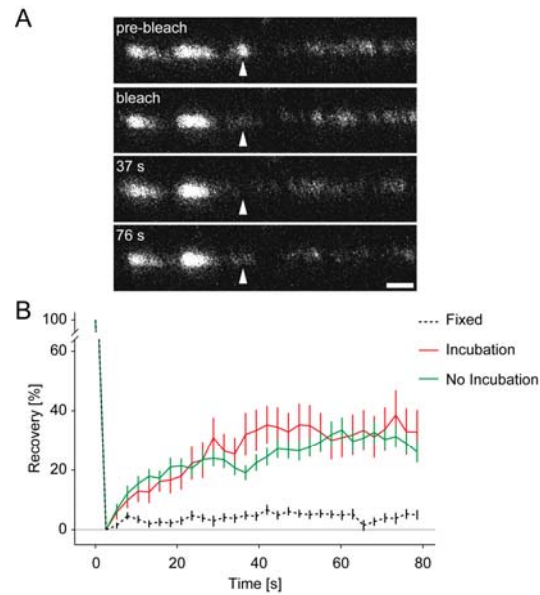


Figure S3: “Fluorescence recovery after photobleaching (FRAP) before and after incubation”

(A) Confocal microscopy images during a FRAP experiment on a hippocampal neuron shortly (12 minutes) after anti-synaptotagmin staining. The bleached region (arrowhead) shows some fluorescence recovery over time, indicating that unbleached synaptic vesicles are moving (inter-synaptically) into the bleached region. Scale bar 1 μ m.

(B) Quantification of fluorescence recovery. The fluorescence recovery was corrected for bleaching during imaging. As control we used fixed cells (2% paraformaldehyde, 3% glutaraldehyde, 60 minutes of fixation). Means \pm s.e.m. are shown for 4–7 independent experiments (with typically up to 10 FRAP curves per experiment).

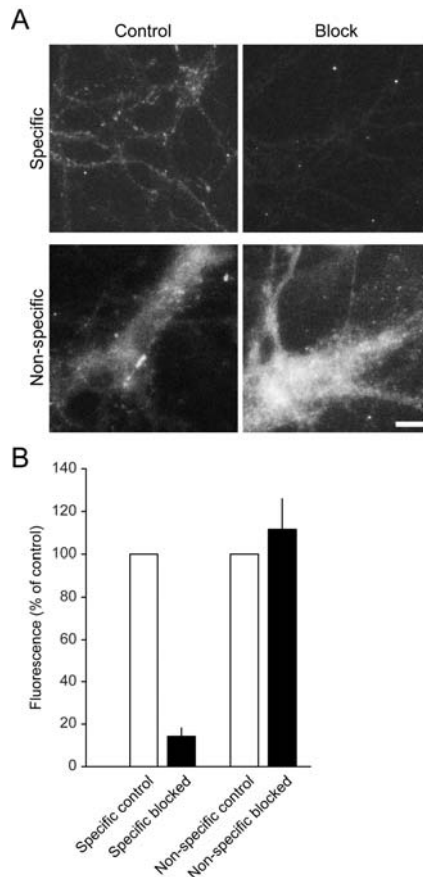


Figure S4: “Specificity of synaptotagmin antibodies labeled with Atto647N”.

Synaptotagmin antibodies (clone 604.2) were labeled with Atto647N in our laboratory by conventional NHS-ester methods. Briefly, the antibodies were purified from ascites fluids by Protein-G-Sepharose binding, eluted from the Sepharose by low pH (2.2), and then coupled with the NHS-ester of Atto647N in presence of 100 mM NaHCO₃. Quenching of the reaction with hydroxylamine was followed by separation from free dye via a Sephadex G25 size-exclusion column. The attempts were not successful, with the antibodies losing specificity, since a substantial proportion of the antibodies were denatured by the low pH treatment, and since the epitope-binding pockets were not protected during labeling. We term these antibodies “non-specific” in this figure.

“Specific” Atto647N-coupled synaptotagmin antibodies (same clone, 604.2) were purchased from Synaptic Systems (Göttingen, Germany).

The specificity and reactivity of the antibodies are tested below.

(A) Hippocampal cultures were incubated with the Atto647N-coupled synaptotagmin antibodies for 15 minutes either without (left panels, control) or with a previous incubation with unlabeled synaptotagmin antibodies (right panels, block). Note that the labeling with the specific antibody disappears due to epitope masking by the unlabeled antibodies, while the non-specific labeling is unaffected. Scale bar 10 μm.

(B) Quantification of the staining. White bars: control staining. Black bars: staining after blocking the epitopes with unlabeled antibodies. Note that the specific labeling is almost eliminated, while the non-specific labeling persists. Means ± s.e.m. are shown from 3 independent experiments, with at least 10 cells analyzed per experiment. Fluorescence intensity was analyzed by manually selecting regions of interest (ROIs), calculating the mean intensity, and subtracting the mean background intensity in neighboring manually selected “empty” ROIs.

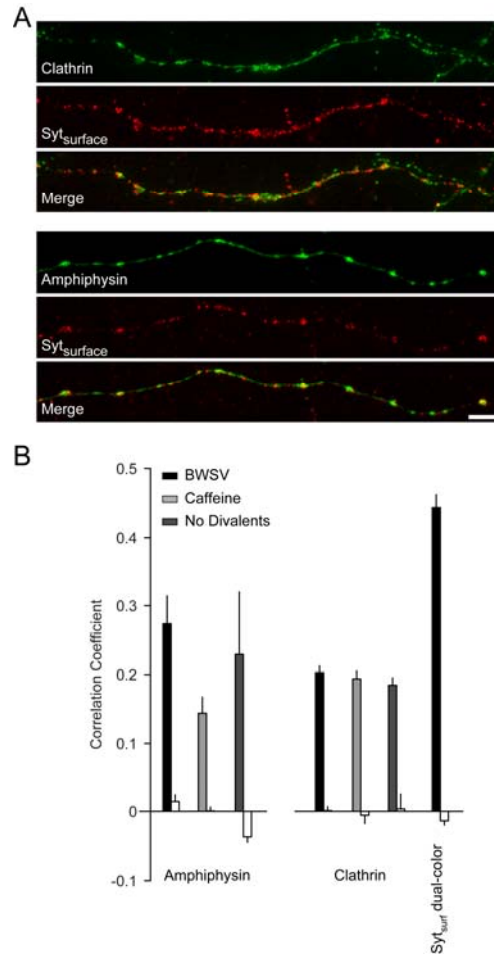


Figure S5: “Correlation between surface synaptotagmin and clathrin machinery components”

(A) Widefield images of the clathrin and surface synaptotagmin distributions. Cultured hippocampal neurons (treated with BWSV) were incubated with primary antibodies against the luminal domain of synaptotagmin and fixed. They were then immunostained (without permeabilization) using Cy5-tagged secondary antibodies (shown in red), before Triton-mediated permeabilization and immunostaining against clathrin or amphiphysin with Cy3-tagged secondary antibodies (shown in green). Scale bar 5 μ m.

(B) Bar graph of the correlation coefficient. Line profiles of fluorescence intensity were performed as in Fig. 2, and the Pearson’s correlation coefficient was obtained for each image pair. A second correlation coefficient, for the intensity line profile in the Cy3 channel with an inversed (mirrored) intensity line profile in the Cy5 channel was also obtained for each experiment (white bars), to give an indication for the random correlation. The control (Syt_{surf} dual-color) indicates the positive control for this experiment (the expected optimal correlation, obtained by immunostaining the surface pool of synaptotagmin with both green (Cy2) and red (Cy5) labeled secondary antibodies). The bars show means \pm s.e.m. from three experiments. The correlation between synaptic vesicle signal and clathrin/amphiphysin is significantly higher than random correlation for the BWSV- and caffeine-treated samples ($p < 0.01$, t-test; $n = 3$ independent experiments; only two independent experiments were analyzed for “No Divalents” samples, for which the error bars show the range of values).

The experiments were performed using an epifluorescence Olympus IX71 microscope equipped with a 1.4 NA, 100 x objective (Olympus), an F-View II CCD camera (Olympus), using standard FITC and Cy5 filters.

Supporting Movie Legends:

Movie S1: Synaptic vesicle motion within an axon. Recently endocytosed synaptic vesicles are shown in red (see text for details on vesicle labeling). Mitochondria (shown in green) are labeled by pre-incubation with 100 nM Mitotracker Green FM. STED (synaptic vesicle) frames were acquired at 28 frames per second; after each 18 frames in the vesicle channel, we acquired two frames in the mitochondria channel (with confocal resolution).

Movie S2: Mobility of synaptic vesicles before and after incubation. STED movies of preparations stained against synaptotagmin, and imaged within 5 minutes (No Incubation, right) or after two hours of incubation (Incubation, left). Movies were acquired at 28 frames per second. To increase the signal-to-noise ratio, the images were filtered as described in Methods.

Movie S3: Influence of stimulation. STED movies of preparations stained against synaptotagmin, and imaged within 10 minutes (No Incubation) or after two hours of incubation (Incubation). After 1.3 seconds of imaging, the preparations were stimulated at 20 Hz for 2 seconds. The movies were processed as for the Movie S2.

Movie S4: Influence of tetrodotoxin. STED movie of a preparation labeled as described and imaged after a 10-minute incubation with 1 μ M tetrodotoxin. The movie was processed as for the Movie S2.

Movie S5: Vesicle material on the surface. STED movies of preparations treated with BWSV, caffeine or incubated shortly in absence of divalent ions, before anti-synaptotagmin labeling and imaging. The movies were processed as for the Movie S2.

Supporting References

1. Willig, K. I., S. O. Rizzoli, V. Westphal, R. Jahn, and S. W. Hell. 2006. STED microscopy reveals that synaptotagmin remains clustered after synaptic vesicle exocytosis. *Nature* 440:935–939.
2. Jahn, R., W. Schiebler, C. Ouimet, and P. Greengard. 1985. A 38,000-dalton membrane protein (p38) present in synaptic vesicles. *Proc Natl Acad Sci USA* 82:4137–4141.
3. Takamori, S., M. Holt, K. Stenius, E. A. Lemke, M. Grønborg, D. Riedel, H. Urlaub, S. Schenck, B. Brügger, P. Ringler, S. A. Müller, B. Rammner, F. Gräter, J. S. Hub, B. L. De Groot, G. Mieskes, Y. Moriyama, J. Klingauf, H. Grubmüller, J. Heuser, F. Wieland, and R. Jahn. 2006. Molecular anatomy of a trafficking organelle. *Cell* 127:831–846.
4. Aguado, F., G. Majó, B. Ruiz-Montasell, J. M. Canals, A. Casanova, J. Marsal, and J. Blasi. 1996. Expression of synaptosomal-associated protein SNAP-25 in endocrine anterior pituitary cells. *Eur J Cell Biol* 69:351–359.
5. Westphal, V., S. O. Rizzoli, M. A. Lauterbach, D. Kamin, R. Jahn, and S. W. Hell. 2008. Video-rate far-field optical nanoscopy dissects synaptic vesicle movement. *Science* 320:246–249.
6. Crocker, J., and D. Grier. 1996. Methods of digital video microscopy for colloidal studies. *Journal of Colloid and Interface Science* 179:298–310.